remote sensing

MDPI

Article

Water–Ecological Health Assessment Considering Water Supply–Demand Balance and Water Supply Security: A Case Study in Xinjiang

Ji Zhang [1], Xiaoying Lai [2,*], Aihua Long [2], Pei Zhang [3], Xiaoya Deng [3], Mingjiang Deng [1], Cai Ren [4] and Yi Xiao [4]

[1] School of Civil Engineering, Tianjin University, Tianjin 300072, China; zhangji940319@tju.edu.cn (J.Z.); xjdmj@tju.edu.cn (M.D.)
[2] College of Management and Economics, Tianjin University, Tianjin 300072, China; aihua_long@tju.edu.cn
[3] China Institute of Water Resources and Hydropower Research, Beijing 100044, China; zhangpei@iwhr.com (P.Z.); dengxy@iwhr.com (X.D.)
[4] College of Water Conservancy & Architectural Engineering, Shihezi University, Shihezi 832000, China; rencai@stu.shzu.edu.cn (C.R.); xiaoyi@stu.shzu.edu.cn (Y.X.)
* Correspondence: xiaoying.lai@tju.edu.cn

Abstract: Water scarcity and ecological degradation in arid zones present significant challenges to regional ecological health. Despite this, integrating the water supply–demand balance and water supply security (SEC) into ecological health assessments—particularly through composite indicators—remains underexplored in arid regions. In this study, we assessed the ecological health changes in Xinjiang by utilizing multivariate remote sensing data, focusing on the balance between water supply and demand, the degree of SEC, and ecosystem resilience (ER). Our results indicate that while water supply and demand remained relatively stable in northern Xinjiang between 2000 and 2020, the conflict between supply and demand intensified in the southern and eastern agricultural regions. SEC evaluations revealed that 73.3% of the region experienced varying degrees of decline over the 20-year period. Additionally, ER assessments showed that 7.12% of the region exhibited a significant decline, with 78.6% experiencing overall reductions in ecological health. The indicators' response to drought demonstrated that improvements in ecological health during wet conditions were less pronounced than declines during droughts. This study underscores the necessity of prioritizing areas with lower ecological health in future water allocation strategies to optimize water resource utilization.

Keywords: ecological health assessment; water supply–demand balance; ecological resilience; water supply security; arid zones

Citation: Zhang, J.; Lai, X.; Long, A.; Zhang, P.; Deng, X.; Deng, M.; Ren, C.; Xiao, Y. Water–Ecological Health Assessment Considering Water Supply–Demand Balance and Water Supply Security: A Case Study in Xinjiang. *Remote Sens.* **2024**, *16*, 3834. https://doi.org/10.3390/rs16203834

Academic Editors: Yeqiao Wang, Zhong Lu, Yongwei Sheng and Yuyu Zhou

Received: 6 September 2024
Revised: 11 October 2024
Accepted: 14 October 2024
Published: 15 October 2024

1. Introduction

With the intensification of global climate change and human activity, the issues of water scarcity and ecological degradation have become increasingly severe [1]. Although the utilization efficiency of surface water resources has been improved to some extent by using water storage projects such as reservoirs and lakes, the contradiction between the supply and demand of water resources in many areas is still acute [2]. This issue is particularly prominent in arid and semi-arid regions, where insufficient water supply significantly impacts ecosystem health [3]. The accurate identification of ecological risks and health conditions is crucial for ensuring the rationality of water supply management [4]. Consequently, scientifically assessing the balance between water supply and demand, as well as ecosystem health, has become a focal point of research, providing a scientific basis for water resource management and ecological protection in arid zones.

Evaluating ecological health offers a new perspective on ecological conservation, and scholars have conducted in-depth research on this topic from multiple angles [5]. These

studies primarily focus on theoretical discussions, practical applications, and exploratory experiments [6]. Since the concept of ecological health was first proposed by Rapport et al. in 1998, scholars have continuously refined its definition. The concept emphasizes that ecosystems should be stable and adaptive, capable of withstanding long-term or sudden natural or anthropogenic disturbances [7]. The emergence of ecosystem services has provided new approaches to ecological health assessment. These services encompass all benefits humans derive from ecosystems, including provisioning, regulating, cultural, and supporting services [8]. Fu et al. synthesized previous research and defined a healthy ecosystem as one characterized by rich biodiversity, resilience to disturbances, structural integrity, self-sustainability, renewability, and the ability to meet human needs while providing societal benefits [9].

Ecological health is critical for sustainable ecological development and harmony between society and the environment [10]. In evaluating methods, researchers have considered hydrology, water quality, watershed characteristics, and watershed services to analyze watershed health, subsequently constructing an evaluation index system. Methods such as TOPSIS [11], principal component analysis, AHP [12], the pressure–state–response (PSR) model [13], and the geometric weighting method [14] have been widely applied in ecological health assessments. For instance, Zhu et al. used the CRITIC objective weighting method to evaluate ecological environment vulnerability in Tianshui city, considering the indicators of ecological, economic, and social development [15]. Similarly, Yue et al. assessed water–ecological construction models in five Chinese cities and ten global cities by considering water resources, the ecological environment, and economic and social development levels [16]. However, a key challenge of these methods is determining the weights of indicator layers. Subjective bias can easily arise when subjective judgments influence weight determination, while objective weighting methods rely on sample data and may not fully capture the importance evaluators place on different indicators.

Another approach involves constructing remotely sensed indices to assess ecological health, such as the remote sensing ecological index (RSEI) [17] and the vigor–organization–resilience (VOR) model [18]. For example, Du et al. evaluated the ecosystem health of Gannan alpine grasslands using RSEI, with model test results showing RSEI's effectiveness in assessing ecosystem health [19]. Sun et al. improved the VOR model to develop a comprehensive ecological health evaluation system for alpine wetlands, successfully applying it to the source area of the Black River [20]. However, most recent studies focus on the ecological health of developed cities and wet environments [21,22], with less attention given to semi-arid and arid zones, where climatic differences make ecosystems more vulnerable to disruption.

In constructing an indicator system, the choice of indicator layers significantly influences the bias of evaluation results [6]. For instance, Hong et al. included total nitrogen and permanganate indices to construct an indicator system to characterize the water–ecological health of the Sunan Canal, providing a more comprehensive and accurate reflection of its current status [23]. Kaghazchi and Soleimani introduced the pollution index of potentially toxic elements in PM2.5 for urban ecology and human health risk assessment [24]. Lei et al. evaluated the ecological patterns, functions, and stresses in aquatic and terrestrial systems within the Qing River Basin [25]. In ecologically fragile arid zones, water is a critical determinant of ecological health [26]. Scholars have attempted to incorporate precipitation and evapotranspiration indicators into ecosystem assessments to address water-related issues [27,28]. Gu et al. developed a river ecosystem health assessment system based on three aspects: water environment, water ecology, and water resources, including water quality, eutrophication, aquatic organisms, and habitat conditions [29]. Their evaluation system objectively reflects river ecological health. Xu et al. quantified water production services in the Shanxi section of the Yellow River Basin using the InVEST model, revealing that population density negatively impacts the trade-off between water supply and demand [30]. Dagnachew Legesse used the dynamic water and chlorine balance model and the watershed hydrological model to discuss the water level and salinity changes of

the tropical lake Abiyata in East Africa under the influence of climate change and human activity and revealed the sensitivity of the lake to environmental changes, indicating that human activity has a significant impact on the lake balance system [31]. However, their study was limited by data availability and did not quantify changes in water balance or the significance of water supply security in vegetation environments, both of which are critical for ecological health evaluation.

Given the research objectives, this study selected Xinjiang as a representative arid region. To minimize inaccuracies in evaluation results caused by subjective indicator selection, this study incorporated the supply–demand ratio of water production services and the degree of water supply security into the RSEI evaluation, aiming to develop a model applicable to the quantitative assessment of ecological health in arid regions. The proposed ecological health evaluation model integrates the supply–demand ratio of water production services, water supply security, and ecosystem resilience. Compared to existing studies, the contributions of this study are as follows: (1) It elaborates on the concept of ecological health evaluation, emphasizing that ecological sub-health consists of multiple subsystems. (2) It explores the spatial distribution characteristics of water production services, water supply security, and ecosystem resilience, integrating their analyses from the perspective of water security. Strategies for sustainably improving ecological health in arid areas are also discussed, offering ideas and references for optimal water resource allocation. (3) It expands the focus area of ecological security research by shifting attention to less-developed regions like western China rather than just coastal areas. (4) It proposes a model adapted to ecological health evaluation in arid areas based on water balance and water supply security, ensuring the objectivity and scientific validity of the evaluation results by avoiding subjective weight allocation.

In summary, this study's objectives and contributions are as follows: (1) From the perspective of water balance and water supply security, we constructed a framework applicable to ecological health assessment in arid zones. The framework incorporates the water supply–demand ratio (WSDR), the degree of water supply security (WSC), and ecological resilience (ER) as key indicators, building an assessment model accordingly. (2) We assessed the changes in these three indicators and the composite indicator between 2000 and 2020, examining patterns of change while considering the impact of drought on the indicators and the assessment system. (3) Based on the ecological health assessment, we propose water supply strategies to policymakers to facilitate the revision and improvement of existing ecological conservation policies and strategies.

2. Materials and Methods

2.1. Study Area

The Xinjiang Uygur Autonomous Region (XUAR) is located in northwestern China, spanning latitudes 34°25′ to 48°10′ north and longitudes 73°40′ to 96°18′ east. This vast area makes Xinjiang the largest provincial-level administrative region in China (Figure 1). Xinjiang's topography is diverse, characterized by the Altai Mountains in the northwest, the Kunlun Mountains in the south, and the Tianshan Mountains in the center, which effectively divide the region into northern and southern parts. The terrain generally rises from the southeast to the northwest, with an average elevation of approximately 2500 m.

Xinjiang experiences a typical temperate continental climate, with cold, dry winters and hot, arid summers. The region's average annual temperature hovers around 10 °C, while the annual precipitation varies significantly, ranging from 50 to 150 mm. This precipitation is mostly concentrated during the summer, while winter is marked by a long snowy season. The average annual precipitation across Xinjiang is 125.1 mm, though there are substantial regional disparities, with southern Xinjiang experiencing higher temperatures and lower precipitation.

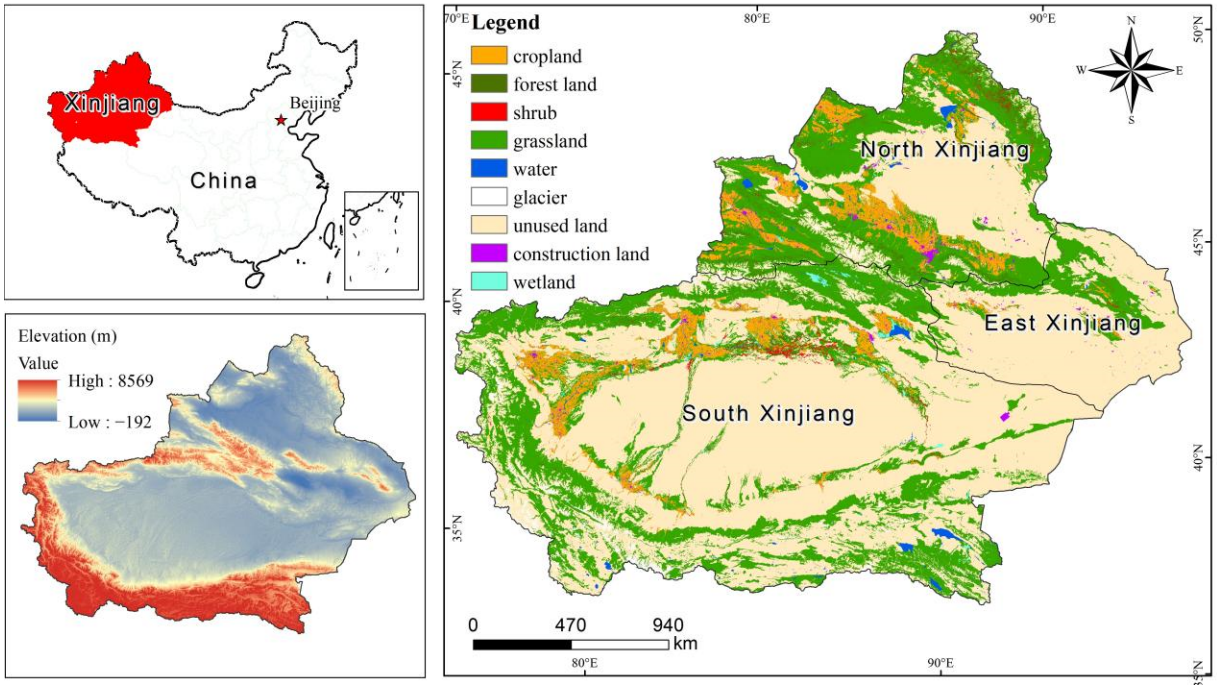

Figure 1. The research area.

The unique geographical location and climatic conditions of Xinjiang have fostered rich natural resources and biodiversity. The region's ecological functions are crucial for maintaining regional ecological balance and promoting harmonious coexistence between humans and nature. Xinjiang holds significant strategic importance for China and, on a global scale, serves as a vital reserve of strategic resources and as an ecological security barrier. However, due to its complex topography, high altitude, cold climate, and low precipitation, Xinjiang is recognized as an ecologically fragile region.

2.2. Data Sources

The data used in this study mainly included meteorological, soil, land use, vegetation, and water resource data (Table 1). The temperature and precipitation datasets were raster data with a 1 km resolution generated by the Delta spatial downscaling scheme in China based on the global 0.5° climate dataset released by CRU and the global high-resolution climate dataset released by WorldClim. These datasets were evaluated using observation data from 496 weather stations [32]. The evapotranspiration data were from the PML-V2 coupled water–carbon land evapotranspiration dataset with a 1 km resolution. The model was calibrated using the parameters from 26 eddy flux stations in China. These data were downloaded from the publicly available dataset of the Tibetan Plateau National Science Data Centre (https://data.tpdc.ac.cn, (accessed 7 May 2024)) and used to drive the InVEST model. The soil moisture dataset was based on the ERA5 reanalysis of climate data downscaled spatially with a spatial resolution of 1 km and a month-by-month temporal resolution. The data can be downloaded from the National Earth System Science Data Centre (https://auth.geodata.cn/, (accessed 8 May 2024)). The soil type data comprised a 1 km raster dataset, and the land use data comprised a 30 m resolution raster dataset, which can be openly accessed at the Data Centre for Resource and Environmental Sciences of the Chinese Academy of Sciences (https:///auth.geodata.cn/, (accessed on 8 May 2024)) (http://www.resdc.cn, (accessed on 8 May 2024)). The surface water resources and water resource quantity data for Xinjiang were obtained from official statistics (http://slt.xinjiang.gov.cn (accessed on 14 May 2024)).

Table 1. Description of the dataset.

Classification	Data Name	Resolution	Time Range	Data Source
Climate	Monthly average temperature (°C)	1 km	2000–2020	The National Scientific Data Center on the Tibetan Plateau (https://data.tpdc.ac.cn) (accessed on 6 May 2024)
	Monthly total precipitation (mm)	1 km	2000–2020	
	Monthly actual evapotranspiration volume (mm)	1 km	2000–2020	
	Monthly potential evapotranspiration volume (mm)	1 km	2000–2020	
	Soil humidity	1 km	2000–2020	The National Data Center for Earth System Sciences (https://auth.geodata.cn/) (accessed on 7 May 2024)
Landform	Altitude (m)	30 m		Geospatial Data Cloud (https://www.gscloud.cn) (accessed on 7 May 2024)
Soil	Type	1 km		Data Center for Resources and Environmental Sciences, Chinese Academy of Sciences (http://www.resdc.cn) (accessed on 8 May 2024)
Land use	Land use type	30 m	2000, 2010, 2020	
Water supply guarantee	Water frequency	30 m	2000, 2010, 2020	Google Earth Engine Platform (JRC, MOD09A1, MOD13A1, MOD11A2) (https://earthengine.google.com/) (accessed on 12 May 2024)
Ecological resilience	NDVI, WET, LST, NDBSI, EVI, LAI	500 m	2000, 2010, 2020	
Water resource data	Surface water resources and production, water system number		2001–2020	Xinjiang Water Resources Department (http://slt.xinjiang.gov.cn) (accessed on 14 May 2024)

In addition to the above publicly available datasets, the water body distribution, normalized difference vegetation index (NDVI), WET, land surface temperature (LST), normalized difference built-up and bareness index (NDBSI), enhanced vegetation index (EVI), and leaf area index (LAI) were obtained from shared datasets on the Google Earth Engine Platform (GEE Platform). The JRC dataset classifies water bodies into non-water bodies (mainly marshes and wetlands), seasonal water bodies (water bodies that do not occur more frequently than every 12 months, seasonal water surfaces, and rivers), and permanent water bodies (water bodies that occur all 12 months of the year, including reservoirs, lakes, and rivers with water all year round) [33]. The resolution accuracy of the seasonal water body data exceeds 98.4%, and that of the permanent water body data exceeds 99.5%, providing a better description of the degree of security of the regional water supply. NDVI, WET, LST, and NDBSI are the four key indicators for calculating the resilience of the data, derived from the waveform calculations of MOD09A1, MOD13A1, and MOD11A2. The calculation method is described in Section 2.3.3, with a resolution of 500 m. EVI and LAI are MODIS product data with a resolution of 500 m, which are used in the validation of water–ecological indicators.

For the simulation output, the water production in the water production simulation at low resolution may over- or underestimate the water production in local areas because the input data do not accurately provide details of the effect of local meteorological conditions on water production. Similarly, we have found in other studies that data of too high a resolution can instead lead to discrimination, e.g., 1 km accuracy resolution data are usually suitable for better results than 30 m resolution LULC data and reduce processing and calibration efforts, thus saving time and resources. We chose a 500 m resolution because it offers higher spatial detail compared to the 1 km and the original 50 km resolutions. This makes the output results more spatially detailed, and the water yield variations are better captured at this resolution [34]. In order to avoid errors in the experimental results caused

by different data resolutions, Arcgis 10.2 was used to resample different raster datasets, and the resolution of the dataset was 500 m after final unification.

2.3. Framework for Assessing the State of Water–Ecological Safety and Health

This study proposes a framework for assessing water–ecological health (WEH) status based on a water-based approach (Figure 2). Based on this, we constructed an index called the water–ecological safety health index (WESHI). The WESHI is based on the calculation of the geometric mean of WSDR and WSC, followed by the introduction of the indicator ER to characterize the stability of water–ecological health. The WESHI aims to measure the specific level of WEH via quantitative analyses. A rasterization approach was used, whereby the study area was divided into small cells and then each raster cell was analyzed using detailed calculations. By calculating the WSDR, WSC, and ER of each raster cell, the WESHI was finally obtained through the below formula to reflect the overall WEH.

$$\mathrm{WESHI} = \left(\frac{\mathrm{WSDR} \times \mathrm{WSC}}{2 - \mathrm{ER}}\right)^{1/2} \tag{1}$$

This index was categorized into the following 5 classes using the natural discontinuity method: poor (0 < WESHI < 0.25); fair (0.25 < WESHI < 0.35); moderate (0.35 < WESHI < 0.45); good (0.45 < WESHI < 0.55); excellent (0.55 < WESHII).

2.3.1. Water Supply–Demand Ratio

The extent of the imbalance between water supply and demand can be quantified using the WSDR for water-producing services, which reflects the proportionality of water supply to water demand in a basin.

The calculation of water supply relies on the water supply–demand module of the InVEST model, which is based on the principle of water balance and estimates water production at the raster level by subtracting actual evapotranspiration (ET) from precipitation (PRE) at the raster scale. The module does not distinguish between surface water, groundwater, and baseflow, but rather assumes that the amount of water produced at each raster feeds into the watershed outlet by way of subsurface or surface runoff. The core algorithm is described below [30].

$$Y_{xj} = \left(1 - \frac{AET_{xj}}{P_x}\right) \times P_x \tag{2}$$

$$\frac{AET_{xj}}{P_x} = \frac{1 + \omega_x + R_{xj}}{1 + \omega_x R_{xj} + (1/R_{xj})} \tag{3}$$

$$\omega_x = Z \times \frac{PAWC_x}{P_x} \tag{4}$$

$$R_{xj} = \frac{k_{ij} \times ET_0}{P_x} \tag{5}$$

where Y_{xj} is the average annual water yield of raster cell x on land use type j; AET_{xj} is the annual actual ET of land use type i on raster x; P_x is the annual precipitation on raster x; R_{xj} is the Budyko dryness index of raster cell x on land cover type j (see Table A1 for details); ω_x is the ratio of the annual available water of modified vegetation to the expected precipitation; Z is the Zhang coefficient [35]; PAWC is the plant available water content; k is the plant ET coefficient. Based on the simulation accuracy, the final Z value was 1.8, meaning that the water production is in line with reality (see Appendix A Figure A1). The simulated water production levels in 2000, 2010, and 2020 were 89.80, 102.18, and 77.84 billion m^3, respectively, which differ by 0.2%, 3.88% and 2.47% compared the total surface water values of 89.69, 106.30, and 76.00 billion m^3 in the same year.

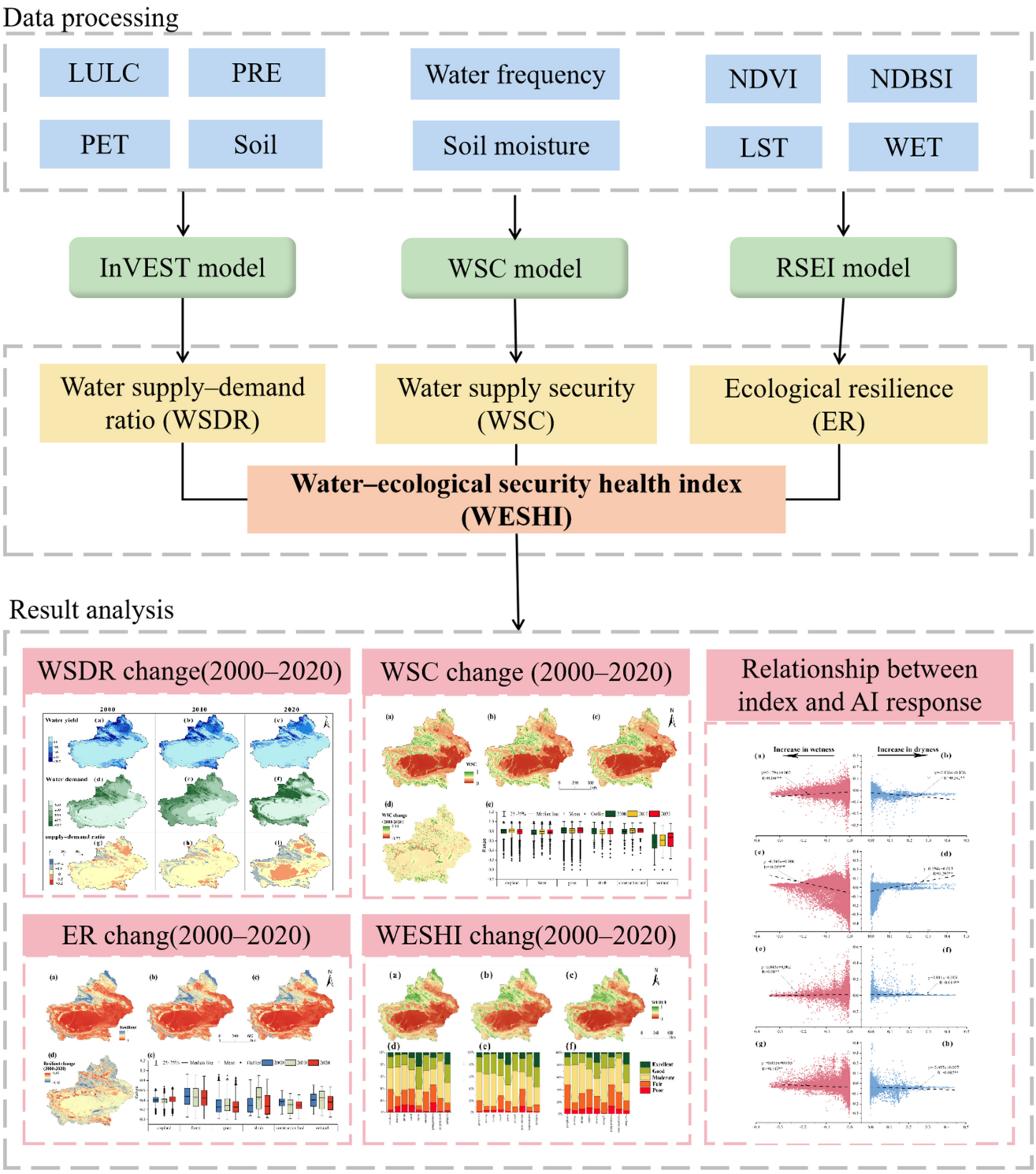

Figure 2. The framework of this study.

The calculation of water demand combines the water demand of human activity with the water demand of vegetation [36]. The water demand for human activity was calculated based on combined per capita water use and population density raster data. As for the water demand of vegetation, it was determined using the modified Penman's formula method, which involves calculating the potential ET of plants and combining the vegetation

coefficient with the soil limitation coefficient in order to derive the actual water demand of plants [37]. The specific formula is shown below.

$$D_w = D_{pwc} \times \rho_{pop} + D_{pwr} \tag{6}$$

$$D_{pwr} = ET_k \times A_k \tag{7}$$

$$ET_k = ET_0 \times K_s \times K_c \tag{8}$$

$$ET_0 = \frac{0.408\Delta(R_n - G) + r\frac{900}{T+273}u_2(e_s - e_a)}{\Delta + r(1 + 0.34u_2)} \tag{9}$$

where D_w is the water demand (m^3); D_{pwc} is the annual per capita water consumption (m^3); ρ_{pop} is the raster population density (person/km^2); D_{pwr} is the total ecological water demand of vegetation (m^3); ET_k is the water demand quota of the kth planted vegetation (mm); A_k is the area of the kth planted vegetation (m^2); ET_0 is the ET of the reference crop (mm); K_s is the soil moisture limitation coefficient of vegetation, with the average value of 0.36 taken in this study; K_c is the vegetation coefficient of the kth planting; Δ is the slope of the saturated water vapor pressure curve (kPa/°C); R_n is the net radiation from the crop surface ($MJm^{-2}day^{-1}$); G is the soil heat flux ($MJm^{-2}day^{-1}$); γ is the moisture table constant (kPa/°C); u_2 is the wind speed at a 2 m height (m/s); e_s is the saturated water vapor pressure (kPa); e_a is the actual water vapor pressure (kPa).

The calculated water demand and supply for each grid was finally brought into the following equation and the metrics were normalized to obtain the supply–demand ratio for each unit of produced water service:

$$WSDR_n = \frac{S_n - D_n}{(S_{max} + D_{max})/2} \tag{10}$$

$$WSDR = \frac{WSDR_n - WSDR_{min}}{WSDR_{max} - WSDR_{min}} \tag{11}$$

where $WSDR_n$ denotes the supply–demand ratio for water production services for the nth land use type, where positive values indicate that the water supply is greater than the water demand, while negative values indicate that the water supply is lower than the water demand [38]; S_n denotes the amount of water supplied for the nth land use type (m^3); D_n denotes the amount of water demanded for the nth land use type (m^3); S_{max} denotes the maximum value of the supply for the land use type (m^3); D_{max} denotes the maximum value of the demand for the land use type (m^3).

2.3.2. Water Supply Security

Water is necessary to maintain the survival of vegetation, and whether vegetation can obtain enough water to maintain its health depends largely on the distance to water sources. We extracted the frequency of occurrence of water bodies in 2000, 2010, and 2020 in the Xinjiang region through the GEE platform, and the water bodies were classified into permanent, seasonal, and other water bodies based on the frequency of occurrence (see Appendix A Figure A2). Different weights were assigned to different water bodies considering the difference in the time they could supply water to the vegetation. Distance rasters for different water bodies were obtained from the Arcgis 10.2 Euclidean distance tool. Soil moisture was introduced into the calculation of water supply security, since it has an important effect on plant growth. Finally, these metrics were normalized in order to obtain the water supply security index by means of the specific formula described below.

$$WSC_0 = 0.7\frac{1}{L_1} + 0.3\frac{1}{L_2} + 0.1\frac{1}{L_3} + \alpha SM \quad (12)$$

$$WSC = \frac{WSC_0 - WSC_{min}}{WSC_{max} - WSC_{min}} \quad (13)$$

where WSC_0 is the degree of water supply security (dimensionless) per unit grid; L_1 is the distance from a permanent water body (km); L_2 is the distance from a seasonal water body (km); L_3 is the distance from other water bodies (km); α is the weight coefficient, which takes the value of 2 in this case; SM is the soil moisture (m^3/m^3); WSC is the water supply security index; WSC_{min} is the minimum value of water supply security; WSC_{max} is the maximum value of water supply security. The value of WSC ranges from [0–1], with larger values indicating a higher degree of water supply security.

2.3.3. Ecological Resilience

The concept of ecological resilience refers to the ability of an ecosystem to absorb disturbances and maintain or recover to its initial state when it encounters various external disturbances and internal changes. This ability is manifested in the ecosystem's ability to cope with the impacts of natural and anthropogenic factors through self-regulation and restoration mechanisms in order to maintain the stability and continuity of its structure and function [9]. This study was conducted by constructing an RSEI indicator to reflect the resilience of ecosystems. The index covers elements such as greenness, humidity, dryness, and heat. Therefore, RSEI can effectively reflect the environmental quality of ecosystems, which is of vital significance for ecosystems to recover from unexpected disturbances and maintain their stability. The specific calculation formula is as follows:

$$RSEI = f(NDVI, WET, LST, NDBSI) \quad (14)$$

where NDVI represents the greenness index of the study area (the NDVI in MOD13A1 was used in this study); WET represents the humidity index of the study area, which reflects the humidity of the water body, soil, and vegetation [39]; LST surface temperature represents the heat index of the study area (the LST index in MOD11A2 was used in this study); NDBSI represents the dryness index of the study area, which is a combination of the soil index (SI) and index-based built-up index (IBI), which can reflect the degree of dryness of the surface of an area [40]; f is the principal component analysis (PCA) method [41], which is a multivariate statistical method that automatically and objectively determines the weights of each indicator based on the nature of the data used and the contribution of the four indicators mentioned above to each principal component, thus avoiding the resultant bias of human subjective factors in the weight-setting process [42].

$$WET = 0.1147\rho_1 + 0.2489\rho_2 + 0.2408\rho_3 + 0.3132\rho_4 - 0.3122\rho_5 - 0.6416\rho_6 - 0.5087\rho_7 \quad (15)$$

$$NDBSI = (SI + IBI)/2 \quad (16)$$

$$SI = \frac{(\rho_6 + \rho_1) - (\rho_2 + \rho_3)}{(\rho_6 + \rho_1) + (\rho_2 + \rho_3)} \quad (17)$$

$$IBI = \frac{(2\rho_6/(\rho_6 + \rho_2)) - (\rho_2/(\rho_2 + \rho_1)) - (\rho_4/(\rho_4 + \rho_6))}{(2\rho_6/(\rho_6 + \rho_2)) + (\rho_2/(\rho_2 + \rho_1)) + (\rho_4/(\rho_4 + \rho_6))} \quad (18)$$

where ρ_1–ρ_7 are bands 1–7 in the MOD09A1 image dataset, corresponding to the red band, near-infrared 1 band, blue band, green band, near-infrared 2 band, short-wave infrared 1 band, and short-wave infrared 2 band, respectively.

Finally, the above four natural metrics were removed from the scale and their values were mapped to the [0, 1] interval using Equation (19). The first principal component (PC1)

can be obtained using the principal component analysis module, followed by the initial ecological index; then, the RSEI of the image elements can be obtained using Equation (20) [43].

$$NI_i = (I_i - I_{min}) / (I_{max} - I_{min}) \quad (19)$$

$$RSEI_i = (PC1 - PC1_{min}) / (PC1_{max} - PC1_{min}) \quad (20)$$

$$ER = (RESI_0 - RESI_{0min}) / (RESI_{0max} - RESI_{0min}) \quad (21)$$

where the value of ER is [0, 1], and $RESI_{0min}$ and $RESI_{0max}$ are the maximum and minimum values of $RESI_0$, respectively. If the value of ER is closer to 1, it means that the ER state is better, while a value of ER closer to 0 means that the ER state is worse.

2.4. Aridity Index

The aridity index (AI) is an indicator calculated based on the ratio of potential evapotranspiration (PET) to precipitation, designed to assess the aridity of a given region [44]. By calculating the ratio of these two parameters, an index reflecting the drought status of the region can be derived, which in turn helps to understand in depth and evaluate the climate characteristics of the region. This study was based on the month-by-month potential evapotranspiration (PET) and precipitation (PRE) over 1 km in China, and the ratio method was used to obtain the formula (AI = annual PET/annual PRE). AI is an index characterizing the degree of wetness and dryness of a region, and based on the classification of AI, the region can be broadly classified into humid (AI < 1, equivalent to forests), semi-humid (AI = 1–1.5, equivalent to forest steppes), semi-arid (AI = 1.5–4, equivalent to steppes), and arid regions (AI $\geq$ 4, equivalent to deserts) [45].

2.5. Rate of Change

The rates of change in the AI (AI_{rate}), water–ecological security health index ($WESHI_{rate}$), supply–demand ratio of water production services ($WSDR_{rate}$), degree of water supply security (WSC_{rate}), and ecological resilience (ER_{rate}) between the periods of 2000–2010 and 2010–2020 were computed using Equations (22)–(26) [44].

$$AI_{rate} = (AI_{2020–2010} - AI_{2000–2010}) / AI_{2000–2010} \quad (22)$$

$$WESHI_{rate} = (WESHI_{2020–2010} - WESHI_{2000–2010}) / WESHI_{2000–2010} \quad (23)$$

$$WSDR_{rate} = (WSDR_{2020–2010} - WSDR_{2000–2010}) / WSDR_{2000–2010} \quad (24)$$

$$WSC_{rate} = (WSC_{2020–2010} - WSC_{2000–2010)} / WSC_{2000–2010} \quad (25)$$

$$ER_{rate} = (ER_{2020–2010} - ER_{2000–2010}) / ER_{2000–2010} \quad (26)$$

3. Results

3.1. Analysis of Spatial and Temporal Variations in WSDR

The analysis of water production in Xinjiang across the years 2000, 2010, and 2020 (Figure 3a–c) revealed a significant disparity between the northern mountainous areas and the rest of the region. Specifically, water production in the Altai and Tianshan Mountains consistently exceeded 200 mm, whereas in the southern and eastern regions, it remained below 50 mm. In terms of water demand (Figure 3d–f), there was a marked increase over the 20-year period, particularly in the oasis agricultural areas of the south and east. These regions, which had water demands below 100 mm in 2000, saw a rise to over 400 mm by

2020. This shift highlights the growth of agricultural development in these areas, along with the heightened pressure on water resources.

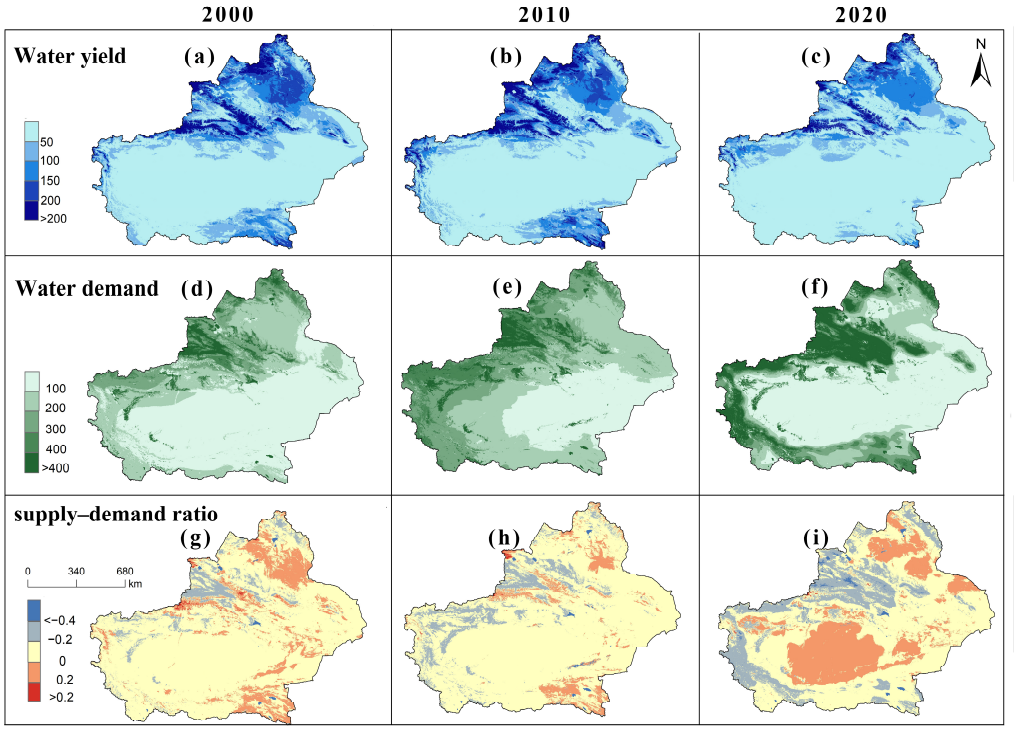

Figure 3. Temporal and spatial distribution of the water supply, water production, and supply–demand ratio in Xinjiang (resolution of 500 m) from 2000 to 2020: water supply (**a**–**c**); water demand (**d**–**f**); supply–demand ratio (**g**–**i**).

The WSDR distribution (Figure 3g–i) shows that the northern region consistently maintained a positive value (>0.2) due to abundant water resources and a sparse population. In contrast, the agricultural regions in the south and east, where water demand far exceeds supply, exhibited negative WSDR values, particularly at the edge of the Taklamakan Desert and the southern foothills of the Tianshan Mountains (<−0.4), indicating severe water shortages. Overall, the northern and mountainous regions of Xinjiang experienced stable water supply and demand, while the southern and eastern agricultural regions faced increasing water stress. Over time, the water resources in the north remained relatively abundant with little change, whereas the conflict between supply and demand in the south and east became more pronounced, particularly in the last decade, during which the area with a negative WSDR expanded.

Between 2000 and 2010, precipitation in Xinjiang increased by 12.5%, from 119.74 to 134.74 mm (Figure 4a). However, in the subsequent decade, precipitation decreased by 19.3%. Potential evapotranspiration (PET) exhibited a significant upward trend from 80.20 mm in 2000 to 109.42 mm in 2020, comprising a 36.4% increase. Actual evapotranspiration (AET) rose from 56.17 mm in 2000 to 70.53 mm in 2010, indicating a 25.5% increase, but then declined by 15.6% to 59.56 mm in 2020. Runoff experienced a slight increase between 2000 and 2010, followed by a significant decrease of 23.4% by 2020.

Most land use types exhibited negative WSDR values, indicating that water supply was lower than demand in these areas (Figure 4b). Notably, the WSDR for grasslands and built-up land decreased steadily over the 20-year period, showing a significant water supply deficit, especially in 2020. The water demand for grasslands increased from 89,040 million m^3 in 2000 to 117,518 million m^3 in 2010, representing a 32% rise, and further increased by 17.6% to 138,226 million m^3 in 2020. The water demand for built-up land nearly doubled from 1316 million m^3 in 2000 to 2627 million m^3 in 2010, but then slightly decreased by 9.9% to 2367 million m^3 in 2020. In contrast, wetlands showed an improved

WSDR in 2020. The WSDR for arable land and woodlands fluctuated less but remained in a negative balance. The water demand for croplands surged significantly from 20,538 million m^3 in 2000 to 33,294 million m^3 in 2010, comprising a 62.1% increase, but decreased slightly by 2.8% to 32,353 million m^3 in 2020.

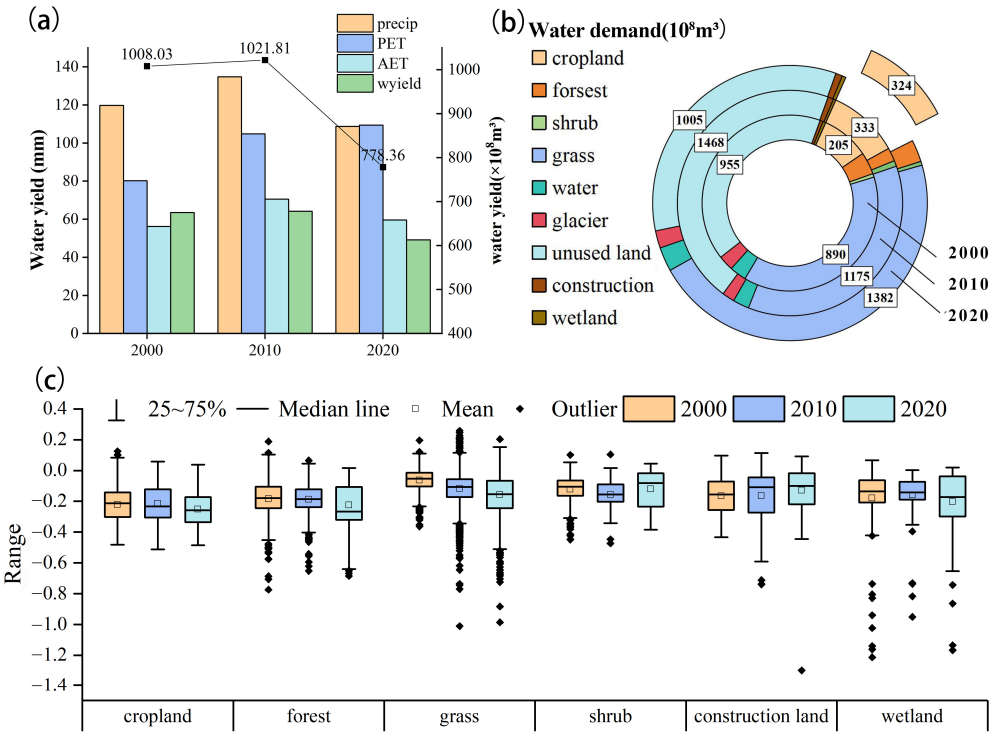

Figure 4. Statistics on the water production, water demand, and WSDR in Xinjiang from 2000 to 2020. Changes in average water production, PRE, total water production, and AET from 2000 to 2020 (**a**); changes in water demand for different land use types from 2000 to 2020 (**b**); changes in WSDR for different land use types from 2000 to 2020 (**c**).

The changes in WSDR across different land types show significant variability (Figure 4c). Agricultural and construction land exhibited the most pronounced declines, likely due to urban expansion and land use changes, while forest and grassland WSDR values remained relatively stable. However, the WSDR of wetlands declined significantly.

3.2. Analysis of the Spatial and Temporal Variations in WSC

High WSC areas were predominantly concentrated around the Taklamakan Desert, the southern foothills of the Tianshan Mountains, and the Ili Valley (Figure 5a–c). These regions have consistently maintained high levels of WSC over the past three decades. In contrast, the Altai Mountains, the northern foothills of the Tianshan Mountains, and some eastern oasis regions displayed lower levels of water supply security. A comparison of changes between 2000 and 2020 revealed that 73.3% of the regions experienced a decrease in WSC, while 36.7% saw an increase (Figure 5d). The areas of high WSC in the southern border regions expanded and became concentrated along the Tarim River mainstream, while WSC in the northern border regions and parts of the east decreased.

The changes in WSC across different land use types from 2000 to 2020 (Figure 5e) indicate that the security of arable and construction land significantly increased, while that of grasslands fluctuated but generally remained stable. Shrublands also remained relatively stable, and wetlands showed an increase in WSC in 2020 but with fluctuations and a broader distribution.

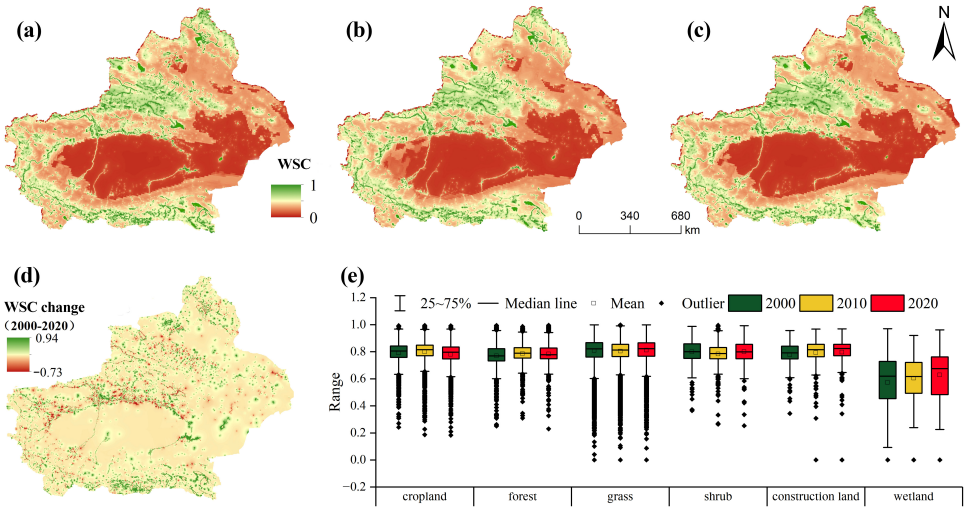

Figure 5. Spatial distribution of the degree of ecological water supply security in Xinjiang from 2000 to 2020 (resolution of 500 m). Spatial distribution of the WSC in 2000, 2010, and 2020 (**a**–**c**); trend of changes in the degree of WSC from 2000 to 2020 (**d**); changes in the WSC of different land use types from 2000 to 2020 (**e**).

3.3. Analysis of the Spatial and Temporal Changes in ER

The distribution of ER in Xinjiang for 2000, 2010, and 2020 (Figure 6a–c) showed a decline in overall mean value from 0.22 to 0.19. Low-resilience regions were concentrated in the Tarim Basin and southern Xinjiang, while areas near the Tianshan and Altai Mountain ranges exhibited relatively higher resilience. The spatial distribution of ER changes from 2000 to 2020 (Figure 6d) indicates that 91.56% of the study area experienced no significant change (±0.1) in resilience. However, 7.12% of the area, primarily near the Tianshan Mountains, saw a more pronounced decline in resilience, while only 1.33% of the area, concentrated around the Taklamakan Desert, exhibited a significant increase in resilience.

The changes in ER across different land use types (Figure 6e) showed that the ER for arable and construction land was narrower and more concentrated, indicating less variability. In contrast, the ER for forests and grasslands was broader, suggesting significant fluctuations in resilience during the study period. Forested land exhibited the highest resilience in 2010, while built-up land consistently showed lower resilience across all time points.

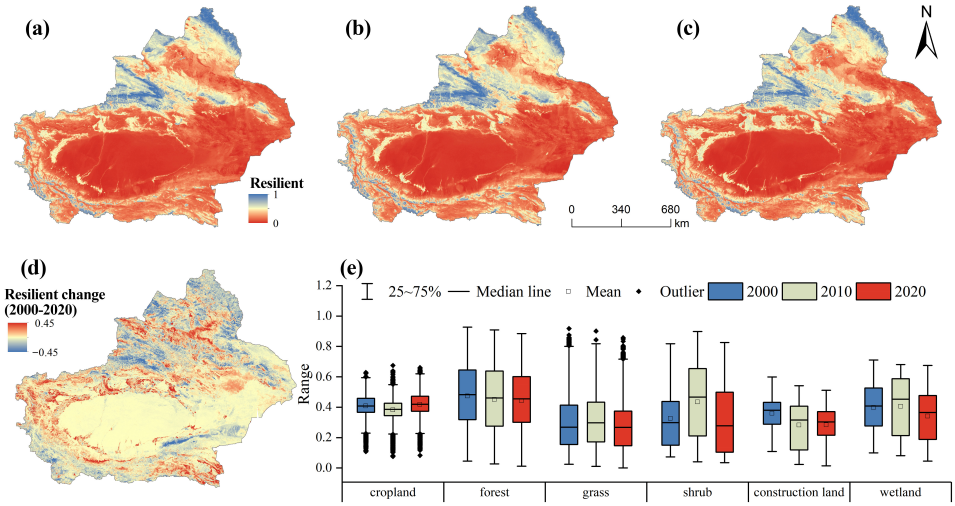

Figure 6. Distribution of ER (**a**–**c**) (resolution of 500 m), changes in ER between 2000 and 2020 (**d**) (resolution of 500 m), and changes in ER by land use type (**e**).

3.4. Evaluation of the WESHI

Between 2000 and 2020, 78.6% of the region experienced a decrease in the WESHI. The averages for the three time points were 0.31, 0.34, and 0.29, respectively, indicating a general decline in ecological health. The spatial and temporal distribution shows that the Tarim Basin and its surrounding areas consistently maintained low WESHI levels, while the areas with high WESHI levels in the Tianshan and Altai Mountains shrank over time (Figure 7a–c). In 2000, 77.43% of the region had a low WESHI (i.e., "poor" and "fair"), which decreased to 67.59% in 2010 but rose again to 76.27% by 2020.

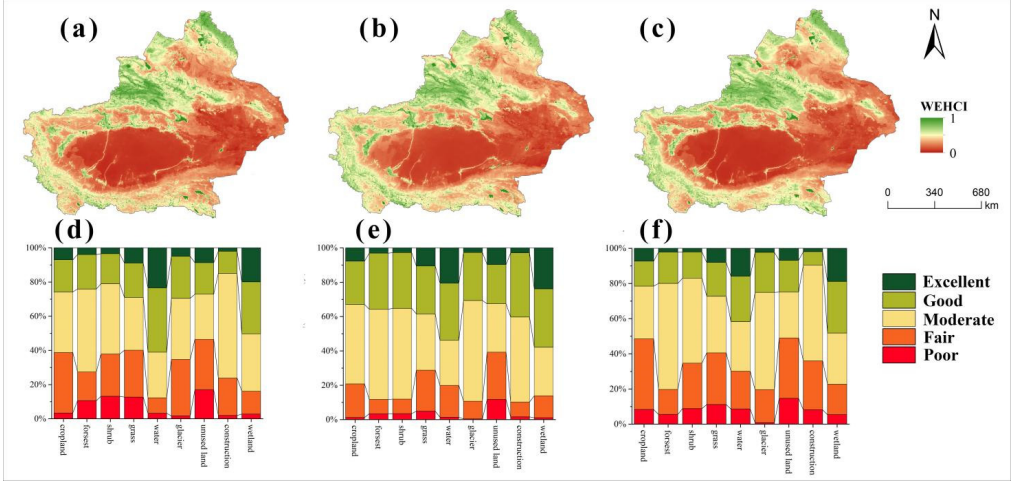

Figure 7. Distribution of the WESHI in 2000, 2010, and 2020 (resolution of 500 m) (**a**–**c**) and different WESHI compositions in 2000, 2010, and 2020 (**d**–**f**).

The health status of various land use types, including cropland, forest, grassland, shrubland, and wetland, showed improvement in 2010 but exhibited a decline by 2020 (Figure 7d–f). The ecological health status of construction land displayed fluctuations, with slight improvements followed by deterioration by 2020. Over the two decades, significant changes were observed in the WESHI across different land use types in Xinjiang. For example, the "poor" status of arable land decreased from 3.32% in 2000 to 1.19% in 2010 but rebounded to 8.34% by 2020. Concurrently, the "good" status increased from 18.81% in 2000 to 25.20% in 2010, before declining to 14.27% in 2020. Woodland areas maintained a high "moderate" status, with percentages of 48.51%, 52.51%, and 60.28% across the three time points. Additionally, the "fair" status of construction land decreased from 21.90% in 2000 to 8.65% in 2010 but increased again to 27.85% by 2020.

Overall, the ecological health of all land use types showed general improvement in 2010, followed by fluctuations in 2020, particularly with significant increases in the proportions of "poor" and "fair" statuses for certain land types. This reflects the pressures and instability faced by the region's ecosystems.

3.5. Indicator Response to AI

In this study, a decrease in the aridity index (AI) was interpreted as an increase in wetness, while an increase in AI signified an increase in dryness. The WESHI rate increased slightly under wet conditions but decreased significantly under dry conditions, with the trend being more pronounced under dry conditions. The rate of change in the WESHI rate continued to increase as the wetting trend decreased, but was always below 0 (Figure 8a). In addition, as the dryness increased, the WESHI rate showed a decreasing trend with a slope of −0.136 (Figure 8b), and the WESHI rate was below 0 in general. This result suggests that the rate of ecological health reduction was greater under dry conditions than under wet conditions.

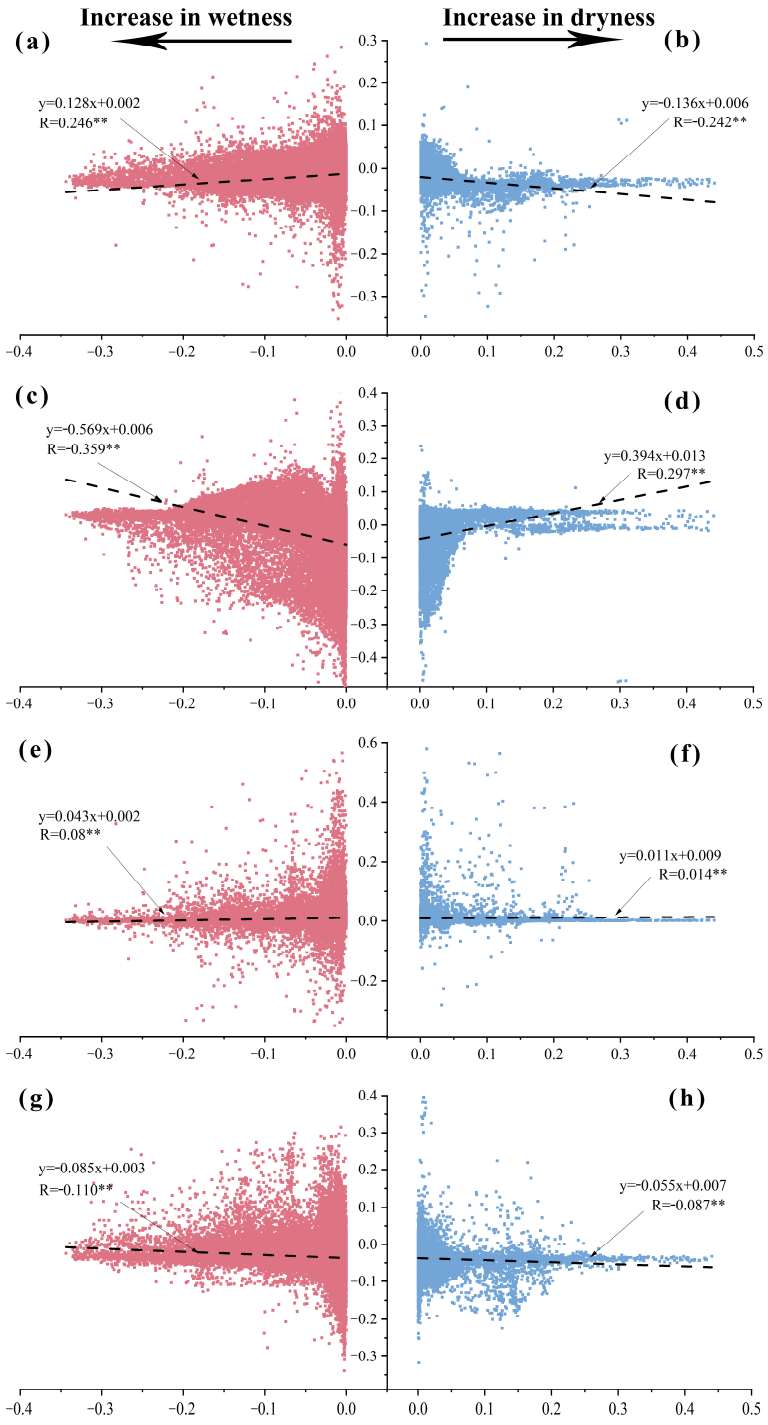

Figure 8. Relationship between indicators and changes in AI (2000–2020): between the WESHI and AI (**a**,**b**); between WSDR and changes in AI (**c**,**d**); between WSC and AI (**e**,**f**); between ER and AI (**g**,**h**). ** denotes passing the 0.01 significance level test.

The WSDR rate increased with increasing humidity, with the turning point at an AI rate of −0.1. WSDR increased significantly when the AI rate was less than −0.1 and decreased when the AI rate was between −0.1 and 0. In contrast, under dry conditions, the WSDR rate increased significantly with increasing dryness (Figure 8c,d). The WSC rate changed little overall, indicating that changes in drought had a limited impact on water supply security (Figure 8e,f). The ER rate had a slope of −0.085 under wet conditions, whereas under dry conditions, it had a slope of −0.055, and the response of ER to wetness was stronger than to drought (Figure 8g,h).

4. Discussion

4.1. Ecological Health Assessment and Changes in the WESHI

This study analyzed the water supply–demand ratio (WSDR), water supply capacity (WSC), ecological resilience (ER), and water–ecological security health index (WESHI) in the Xinjiang region across the years 2000, 2010, and 2020. The results revealed a growing conflict between water supply and demand, uneven water supply security, and a weakening of ecosystem resilience over the past two decades. Specifically, the mountainous areas of northern Xinjiang consistently produced significantly more water than the southern and eastern regions. However, the southern and eastern agricultural regions experienced a sharp rise in water demand over time, leading to a marked deterioration in the supply–demand ratio and a severe shortage of water supply. Although the WSC improved in certain areas along the southern border, the distribution remained uneven, with some regions even witnessing a decline. The overall reduction in ER, particularly in southern Xinjiang, expanded low-resilience areas, highlighting the vulnerability of ecosystems to drought and climate change. This study concludes that the WESHI initially increased and then declined from 2000 to 2020, indicating a deterioration in ecosystem health in response to increasing water stress, particularly in the southern agricultural region and around the Tarim Basin. Imbalances between water supply and demand, coupled with low WSC levels, are critical factors contributing to the decline in ecosystem health. These findings offer a new perspective for future ecological health assessments in arid regions and underscore the significance of water management in ecological conservation.

The results align with previous studies to some extent. For instance, studies by Li et al. in 2017 and Zhang et al. in 2019 similarly reported an intensification of the water supply–demand conflict and increased ecosystem vulnerability in northwest China [46,47]. However, discrepancies were observed when compared side by side with other similar studies. For example, Li's study identified a slight deficit in Xinjiang's water supply and demand, which was mitigated by increased precipitation and reduced irrigation water use [36]. In contrast, the water supply–demand balance index in this study showed more pronounced temporal and spatial fluctuations, with irrigation water use increasing. This study also found significant changes in water supply, water demand, and the WSDR index between 2010 and 2020. First, because of the decrease in water supply, the amount of surface water resources in 2020 compared to 2010 decreased by nearly 30 billion m^3. Second, the expansion of arable land and the increase in population increased the water demand, while the effect of higher temperatures intensified the evaporation effect of vegetation, raising the overall water demand. As a result, more areas of imbalance between water supply and demand appeared in 2020. Additionally, while the WSC improved in the southern regions of Xinjiang, this study did not observe a significant increase in these areas' water supply security. These differences may stem from variations in indicator selection and differences in regional water management policies and climate anomalies across different years.

This study introduced an innovative water supply–demand balance index in constructing the WESHI, providing a more direct reflection of the water supply–demand relationship's impact on ecological health than the traditional pressure–state–response (PSR) framework. Furthermore, we discussed the correlation between the WESHI and vegetation indices such as the enhanced vegetation index (EVI) and the leaf area index (LAI) (Figure 9a,b). The fitting results revealed that the WESHI correlates moderately with EVI (r = 0.608) and LAI (r = 0.579), suggesting that the WESHI effectively reflects vegetation health.

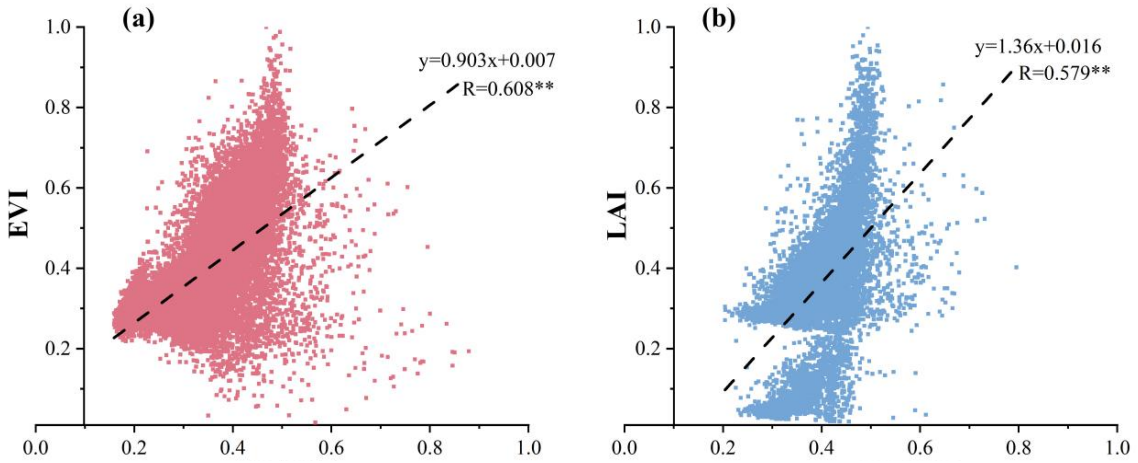

Figure 9. Relationship between the WESHI and the vegetation indices EVI (**a**) and LAI (**b**). ** indicates significant at the 0.01 level. ** denotes passing the 0.01 significance level test.

4.2. Impact of Human Activity on Ecological Health

Human activity has profoundly impacted the ecological health of the Xinjiang region, with both positive and negative consequences [48]. On the positive side, improved water management and irrigation technologies have effectively secured water supply for some cultivated lands [49]. This is particularly evident in the oasis agricultural areas of northern Xinjiang and some key irrigated agricultural areas in southern Xinjiang, where water supply stability has improved [47]. An analysis of the relationship between the expansion of arable land and the WESHI between 2000 and 2020 showed that the expansion of arable land was beneficial to the water ecological health index (the mean value of the change in the WESHI was 0.02) (Figure 10).

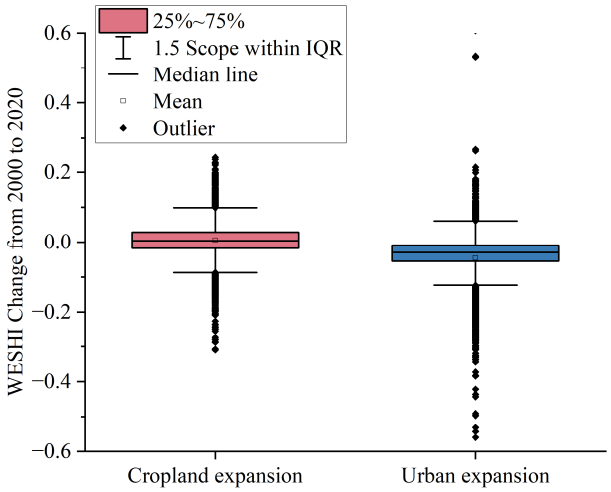

Figure 10. Response of cultivated land and urban expansion to changes in the WESHI between 2000 to 2020.

However, the negative impacts are equally significant. The overexploitation of water resources driven by agricultural expansion and industrial development has led to an imbalance between water supply and demand in many regions [50]. In the arid regions along the southern and eastern borders, massive water abstraction has significantly reduced ecological water use [51]. This reduction in ecological water use has directly led to wetland shrinkage, intensified desertification, and biodiversity loss [52]. At the same time, the expansion of towns and cities accelerated the decline in the WESHI (the change over the last 20 years showed a mean value of −0.05) (Figure 10). Over time, the overuse of water

resources may also lower groundwater levels, exacerbating unsustainable water use and further weakening ecosystems. Additionally, increased human activity has intensified water conflicts between ecological and societal needs, with limited water supply often resulting in ecological water use being squeezed and deteriorating ecosystem health [53].

4.3. Recommendations for Optimal Allocation of Water Resources

Based on this study's results, future water allocation efforts should prioritize regions with low ecological health. These areas tend to be concentrated in the tailrace of the river or far from the river, such as the lower reaches of the Hotan River and parts of the middle reaches of the Tarim River. Such areas are centrally characterized by an imbalance between supply and demand, a low degree of water supply security, and a low degree of resilience, and further neglect may lead to deterioration. Therefore, securing ecological water demand in these regions should be prioritized, and measures should be implemented to alleviate ecosystem pressure and prevent ecological collapse.

In regions with better ecological health, priority levels can be appropriately lowered and existing water management strategies maintained to ensure continued ecosystem health and stability. Additionally, as oasis agricultural areas expand, planning should align with the ecological carrying capacity to avoid new ecological problems arising from excessive development. Through scientifically sound and rational water resource allocation strategies, the sustainability and health of ecosystems can be ensured while maintaining socioeconomic development, thus achieving the coordinated development of water resources and ecological health in the region.

4.4. Impact of Warming and Humidification Processes on the WESHI

Since the beginning of the twenty-first century, experts have pointed to the phenomenon of "warming and humidification" in Xinjiang, which is mainly due to increased temperatures and land surface evaporation, leading to faster water circulation and increased precipitation. Over the past 60 years, the annual rate of surface warming in Xinjiang was 0.30 °C/decade, and the average rate of precipitation increase was 9 mm/decade [54]. Warming and humidification have a significant impact on the water body area in northwest China in terms of interannual change; from 2000 to 2020, the water body area in northwest China increased from 3.48 × 104 to 4.82 × 104 km^2, and the annual rate of change reached 682.64 km^2/a [55]. The expansion of the water body area was more significant in the area along the Tarim River and the western part of Qinghai Province. This strengthens the connectivity between water bodies to a certain extent, enhances the regional WESHI, and is conducive to regional ecological environment construction and protection.

However, the "warming and humidification" process took a turn for the worse after 1997 [56]. Drought trends, frequency, and months in the northwest region increased significantly, resulting in more than 70% of the region drying out, and the phenomenon of the "wet–dry transition" occurred. Increases in temperature increase the actual evapotranspiration, leading to stagnant vegetation growth and a significant decrease in soil moisture, which reduces the degree of water supply security and is not conducive to ecological restoration and protection.

At the same time, the "warming and humidification" process is accompanied by an intensification of extreme weather events, with the risk of further increases in high temperatures and flooding [57]. This poses a great challenge to the use of water resources and disaster prevention and mitigation and places greater demands on agriculture and disaster prevention and mitigation.

4.5. Limitations of This Study

Despite the significant findings of this study, several limitations exist. First, the study data spanned only three years—2000, 2010, and 2020—which may not allow for fully capturing long-term trends. This limited time frame may have led to an incomplete assessment of the long-term impacts of climate change and human activity. Second, this

study primarily relied on remotely sensed data and model simulations. Although the data were resampled to a 500 m resolution for this study, accuracy issues may have still arisen, particularly in areas with complex topography and diverse land use types.

This study only focused on the effect of the frequency of different water bodies on the relationship between the degree of water supply security and the ecological environment and did not consider the response of different types of water bodies, such as reservoirs and lakes, to the quality of the ecological environment. Lakes, as inland water bodies, usually have more stable ecosystems and play a unique role in regulating the climate and maintaining biodiversity. However, lakes are also more vulnerable to human activity, such as pollution and overexploitation, leading to the deterioration of water quality and the degradation of ecological functions. Therefore, when assessing the ecological health of lakes, special attention needs to be paid to water quality, biodiversity, and ecological service functions [58].

Reservoirs, on the other hand, are artificially constructed bodies of water that are mainly used for regulating runoff, flood control, irrigation, and power generation. Compared to lakes, the hydrological characteristics of reservoirs are more complex, and their ecosystems are more susceptible to human regulation [59]. Therefore, when assessing the ecological health of reservoirs, in addition to considering conventional indicators such as water quality and biodiversity, it is also necessary to pay attention to the impacts of the operation and management of reservoirs on the downstream ecosystem.

In addition, there may be differences in the ecological health of different types of lakes and reservoirs. For example, some alpine lakes have relatively fragile ecosystems that are more vulnerable to climate change due to their high altitude and low temperature [60], while some large reservoirs may have more prominent problems, such as eutrophication due to the large capacity of the water body and slow water flow rates [61]. Future research could fully consider the differences between different types of surface water and improve the assessment system through careful categorization and in-depth discussion.

5. Conclusions

This study constructed a water–ecosystem health assessment framework based on the InVEST model and multivariate remote sensing data, systematically assessing the water–ecosystem health status of the Xinjiang region from 2000 to 2020. We focused on quantifying WSDR, WSC, and ER and explored the spatial impacts of drought changes on these indices. The results show the following:

(1) The WSDR indicated a stable water supply and demand situation in the northern and mountainous regions of Xinjiang, while water stress increased in the southern and eastern agricultural regions. The conflict between supply and demand in the southern and eastern regions became more pronounced over time, especially in the last decade, with the area exhibiting an increasing negative supply–demand ratio.

(2) WSC increased in 36.7% of the region to varying degrees between 2000 and 2020, with the area of high water supply security expanding at the southern border, particularly along the mainstem of the Tarim River. However, WSC decreased on the northern border and in some eastern areas.

(3) ER declined in the study area, with the mean ER value decreasing from 0.22 in 2000 to 0.19 in 2020. While 91.56% of the region showed no significant change in resilience ($\pm$0.1), 7.12% exhibited a more pronounced decline, and only 1.33% showed a significant increase in ecological resilience.

(4) The WESHI experienced an initial increase followed by a decline from 2000 to 2020. In 2000, 77.43% of the region had a low WESHI, which decreased to 67.59% in 2010, only to rise again to 76.27% by 2020. The southern Xinjiang region, in particular, experienced an increase in insufficient water supply and ecosystem vulnerability up to 2020.

(5) The WESHI increased slightly under wet conditions but decreased significantly under dry conditions, with the trend being more pronounced under dry conditions. Based on these findings, we recommend strengthening water resource management, enhanc-

ing ecological resilience, and establishing a long-term monitoring and assessment policy. The results not only provide a scientific basis for water resource management and ecological protection in Xinjiang, but also serve as a reference for other regions with similar ecological environments.

Author Contributions: Conceptualization, J.Z. and A.L.; methodology, J.Z.; software, C.R.; validation, J.Z. and P.Z.; formal analysis, A.L.; investigation, X.L.; resources, Y.X.; data curation, A.L.; writing—original draft preparation, J.Z.; writing—review and editing, P.Z.; visualization, X.D.; supervision, M.D.; project administration, A.L.; funding acquisition, X.L. All authors have read and agreed to the published version of the manuscript.

Funding: This research was supported by the National Natural Science Foundation of China (grant nos. 52379020, 52309041, and 52179028) and the Third Xinjiang Scientific Expedition Program (grant no. 2022xjkk0103).

Data Availability Statement: Data will be made available upon request.

Conflicts of Interest: The authors declare no conflicts of interest.

Appendix A

Table A1. Parameters for different land use types in the water production module.

Description	Lucode	Root_depth	Kc	LULC_veg
Cropland	1	2000	0.65	1
Forest	2	5000	1	1
Shrub	3	3500	0.93	1
Grass	4	2000	0.75	1
Water	5	100	1	0
Glacier	6	100	0.5	0
Unused land	7	300	0.2	0
Construction	8	100	0.2	0
Wetland	9	1000	0.8	1

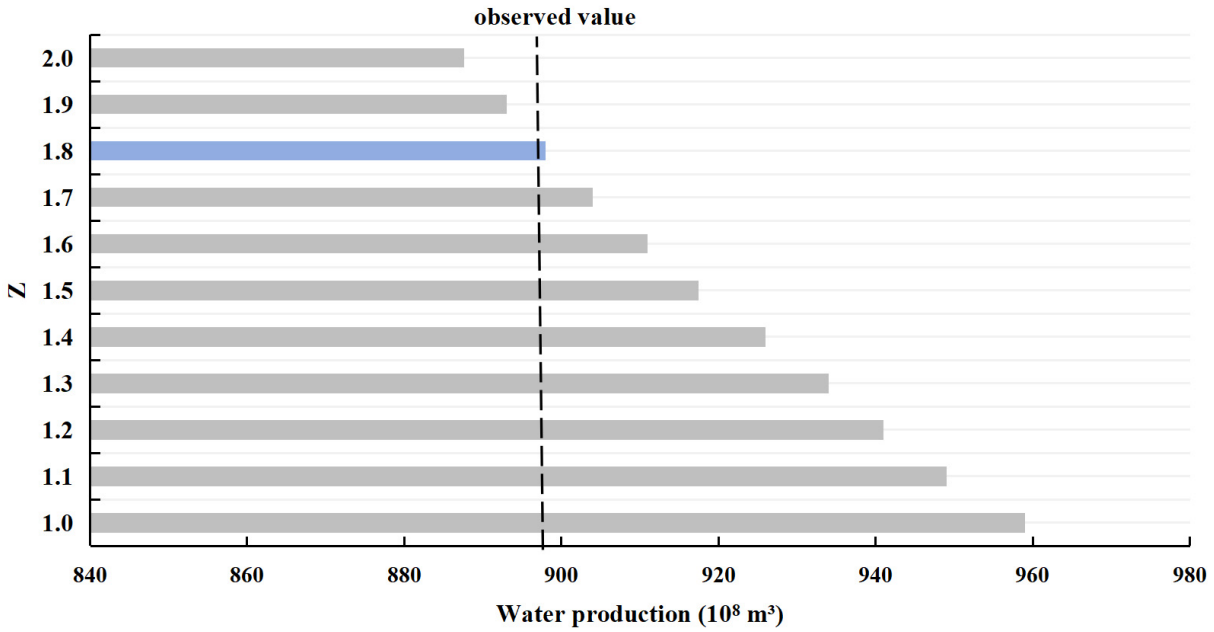

Figure A1. Simulation of water production in the InVEST model at different Z-values (example for the year 2000). Grey indicates the simulated water production at different Z values and blue represents the simulated water production closest to the observed values.

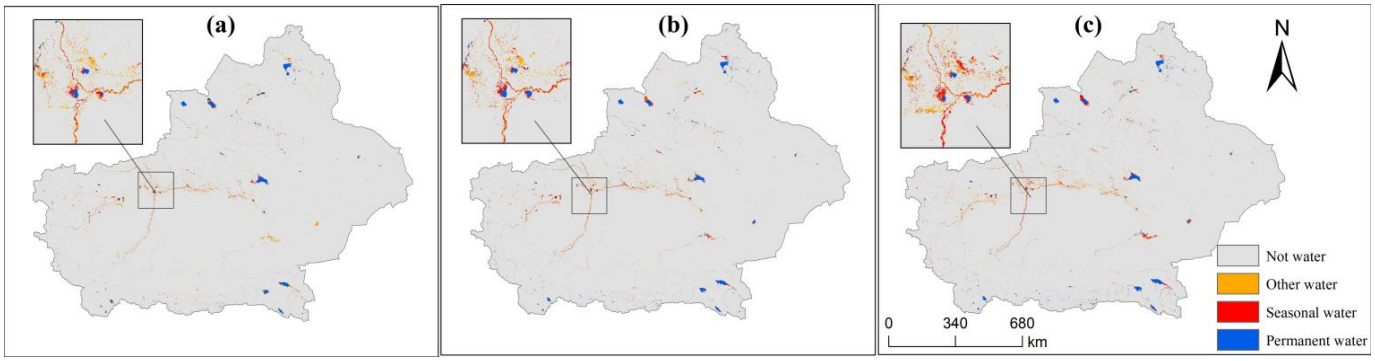

Figure A2. Distribution of water bodies in Xinjiang extracted based on the GEE platform for 2000 (**a**), 2010 (**b**), and 2020 (**c**) (resolution of 30 m).

References

1. Xu, Z.; Wang, J.; Han, J. Ecological Vulnerability Assessment of the Qaidam Basin Based on SRP Model. *J. Salt Lake Res.* **2024**, *32*, 53–60. [CrossRef]
2. Xu, N.; Lu, H.; Li, W.Y.; Gong, P. Natural lakes dominate global water storage variability. *Sci. Bull.* **2024**, *69*, 1016–1019. [CrossRef] [PubMed]
3. Deng, M.; Yang, P.; Zhou, H.; Xu, H. Water Conversion and Strategy of Ecological Water Conveyance in the Lower Reaches of the Tarim River. *Arid Zone Res.* **2017**, *34*, 717–726.
4. Gao, M.; Cai, H.; Zhang, X.; She, Y.; Peng, S. Driving Factors and Evolution of Supply and Demand of Water Conservation Services in Raohe River Basin. *Bull. Soil Water Conserv.* **2024**, *44*, 389–399, 464.
5. Zhang, Z.; Ouyang, H.; Xiao, F.; Sun, J.; Song, D. The current status of ecosystem health and its assessment. *Chin. J. Eco-Agric.* **2004**, *12*, 184–187.
6. Yuan, X.; Liu, H.; Lu, J. Assessment of ecosystem health--concept framework and indicator selection. *Ying Yong Sheng Tai Xue Bao = J. Appl. Ecol.* **2001**, *12*, 627–629.
7. Rapport, D.J.; Costanza, R.; McMichael, A.J. Assessing ecosystem health. *Trends Ecol. Evol.* **1998**, *13*, 397–402. [CrossRef]
8. Guo, Y.; Zhang, S.; Chen, Y. Progress of Ecosystem Health Assessment Study. *Urban Environ. Urban Ecol.* **2002**, *15*, 10–13.
9. Fu, S.; Zhao, L.; Qiao, Z.; Sun, T.; Sun, M.; Hao, Y.; Hu, S.; Zhang, Y. Development of Ecosystem Health Assessment (EHA) and Application Method: A Review. *Sustainability* **2021**, *13*, 11838. [CrossRef]
10. Zhong, R.; Zhong, X.; Yu, G.; He, G. The concept and methods of assessment for regional ecosystem influence of human development and decision. *J. Cent. China Norm. Univ. Nat. Sci. Ed.* **2005**, *39*, 403–408.
11. Wu, S.; Tian, B.; Gu, S.; Yang, L.; Hu, Y. The Influence of Vegetation Coverage on the Dynamic Evolution of Ecological Vulnerability: A Case Study of Zhangjiakou, Hebei Province. *Res. Soil Water Conserv.* **2024**, *31*, 310–320.
12. Cao, R.; Wang, J.; Tian, X.; Zou, Y.; Jiang, M.; Yu, H.; Zhao, C.; Zhou, X. Post-Restoration Monitoring of Wetland Restored from Farmland Indicated That Its Effectiveness Barely Measured Up. *Water* **2024**, *16*, 410. [CrossRef]
13. Dong, W.; Tao, Y.; Pang, Y.; Xu, Q.; Yu, X. Ecological health assessment and main influencing factors of Lake Taihu Basin based on PSR model. *J. Environ. Eng. Technol.* **2024**, *14*, 846–855.
14. Wu, X.; Huang, X. Research on the geometric weighting-coupling degree method for the urban ecological environment vulnerability index. *Ecol. Indic.* **2024**, *162*, 112023. [CrossRef]
15. Zhu, R.; Ao, Z.; Jiang, Y. Assessment of ecological environment vulnerability in Tianshui city based on the CRITIC objective weighting method. *J. Desert Res.* **2024**, *44*, 321–331.
16. Yue, Q.; Heal, K.; Yu, J.; Wang, Q.; Zheng, Y.; Zhu, Z.; Liu, Y.; Xu, S.; Yao, X. The Performance of the Construction of a Water Ecological Civilization City: International Assessment and Comparison. *Sustainability* **2023**, *15*, 3071. [CrossRef]
17. Halder, S.; Bose, S. Comparative study on remote sensing-based indices for urban ecology assessment: A case study of 12 urban centers in the metropolitan area of eastern India. *J. Earth Syst. Sci.* **2024**, *133*, 100. [CrossRef]
18. Lei, D.; Zhang, Y.; Ran, Y.; Gao, L.; Li, J.; Li, Z.; Mo, J.; Liu, X. Assessment of ecosystem health based on landscape pattern in ecologically fragile regions at different spatial scales: A case study of Dianchi Lake basin, China. *Front. Environ. Sci.* **2023**, *11*, 1076344. [CrossRef]
19. Du, Z.; Ji, X.; Liu, J.; Zhao, W.; He, Z.; Jiang, J.; Yang, Q.; Zhao, L.; Gao, J. Ecological health assessment of Tibetan alpine grasslands in Gannan using remote sensed ecological indicators. *Geo-Spat. Inf. Sci.* **2024**, 1–9. [CrossRef]
20. Sun, W.; Qiao, B.; Yu, H.; Zhao, T.; Chen, Q. Ecological health assessment of the alpine wetland landscape in the Heihe River source area based on vigor, organization, and resilience. *Arid Zone Res.* **2024**, *41*, 301–313.
21. Yang, R.; Chen, Y.; Qiu, Y.; Lu, K.; Wang, X.; Sun, G.; Liang, Q.; Song, H.; Liu, S. Assessing the Landscape Ecological Health (LEH) of Wetlands: Research Content and Evaluation Methods (2000–2022). *Water* **2023**, *15*, 2410. [CrossRef]
22. Yang, Y.; Cao, H.; Xia, Y.; Liu, D.; Liu, Y.; Qiao, J. Assessing ecological health in a semi-arid basin: A case study of the Wei River Basin, China. *Environ. Sci. Pollut. Res.* **2024**, *31*, 21687–21708. [CrossRef] [PubMed]

23. Hong, Y.; Wang, D.; Wang, Z.; Chen, Q.; Huang, Y.; Liu, D.; Zhu, Q.; Yan, D.; Lu, H. Identification of key indicators of water ecological health and establishment of comprehensive evaluation system of the Sunan Canal. *Acta Sci. Circumstantiae* **2023**, *43*, 407–417.
24. Kaghazchi, M.E.; Soleimani, M. Changes in ecological and health risk assessment indices of potentially toxic elements associated with ambient air particulate matters (PM2.5) in response to source, land use and temporal variation in Isfahan city, Iran. *Urban Clim.* **2023**, *49*, 101520. [CrossRef]
25. Lei, J.; Zhang, J.; Li, P.; Zhang, H.; Xu, C. Ecological health assessment of the Qinghe River Basin: Analysis and recommendations. *J. Water Clim. Chang.* **2024**, *15*, 868–882. [CrossRef]
26. Xu, D.C.; Wang, X.; Liu, J.Z.; Hu, M.X.; Tian, J.J.; Zhao, H.Z.; Ren, H.Z. Analysis of the spatial and temporal evolution of water and soil resource carrying capacity in arid region of northwest China. *Water Supply* **2022**, *22*, 8813–8834. [CrossRef]
27. Xie, W.; Zhao, X.; Fan, D.; Zhang, J.; Wang, J. Assessing spatio-temporal characteristics and their driving factors of ecological vulnerability in the northwestern region of Liaoning Province (China). *Ecol. Indic.* **2024**, *158*, 111541. [CrossRef]
28. Xu, C.; Hu, X.; Liu, Z.; Wang, X.; Ren, Z.; Zi, Y. Analysis on evolution of carrying state of water and soil resources in artificial oases in arid areas. *J. Drain. Irrig. Mach. Eng.* **2023**, *41*, 62–69.
29. Gu, X.; Wang, Z.; Zhao, X.; Gao, K.; Luo, N.; Mei, P.; Zhang, Z. Establishment and Application of the Index System for River Ecosystem Health Assessment. *Environ. Monit. China* **2023**, *39*, 87–98.
30. Xu, M.; Feng, Q.; Lyu, M. Tradeoffs of ecosystem services and their influencing factors: A case study of the Shanxi Section of the Yellow River Basin. *Arid Zone Res.* **2024**, *41*, 467–479.
31. Legesse, D.; Vallet-Coulomb, C.; Gasse, F. Analysis of the hydrological response of a tropical terminal lake, Lake Abiyata (Main Ethiopian Rift Valley) to changes in climate and human activities. *Hydrol. Process.* **2004**, *18*, 487–504. [CrossRef]
32. Peng, S.; Ding, Y.; Liu, W.; Li, Z. 1 km monthly temperature and precipitation dataset for China from 1901 to 2017. *Earth Syst. Sci. Data* **2019**, *11*, 1931–1946. [CrossRef]
33. Pekel, J.-F.; Cottam, A.; Gorelick, N.; Belward, A.S. High-resolution mapping of global surface water and its long-term changes. *Nature* **2016**, *540*, 418–422. [CrossRef]
34. M'Barek, S.A.; Bouslihim, Y.; Rochdi, A.; Miftah, A. Effect of LULC data resolution on hydrological and erosion modeling using SWAT model. *Model. Earth Syst. Environ.* **2023**, *9*, 831–846. [CrossRef]
35. Wei, P.; Wu, M.; Jia, Y.; Gao, Y.; Xu, H.; Liu, Z.; Chen, S. Spatiotemporal variation of water yield in the upstream regions of the Shule River Basin using the InVEST Model. *Acta Ecol. Sin.* **2022**, *42*, 6418–6429.
36. Li, F.; Li, Y.; Zhou, X.; Yin, Z.; Liu, T.; Xin, Q. Modeling and analyzing supply-demand relationships of water resources in Xinjiang from a perspective of ecosystem services. *J. Arid Land* **2022**, *14*, 115–138. [CrossRef]
37. Zhu, W.; Zhang, Z.; Guo, X.; Feng, S.; Jiang, D.; Jiang, F. Characteristics and estimation of vegetation ecological water demand in the Mara River Basin. *Acta Ecol. Sin.* **2023**, *43*, 7523–7535.
38. Zhang, C.; Sun, X.; Zhang, H.; Deng, C.; Zhao, K.; Jin, Y.; Chen, D. Supply-Demand Balance of Ecosystem Services in the Middle Reaches of the Yangtze River Based on Land Use Change. *J. Soil Water Conserv.* **2024**, *38*, 227–238.
39. Xiao, F.; OuYang, H.; Fu, B.; Niu, H. Forest Ecosystem Health Assessment Indicators and Application in China. *Acta Geogr. Sin.* **2003**, *58*, 805–809.
40. Lobser, S.E.; Cohen, W.B. MODIS tasselled cap: Land cover characteristics expressed through transformed MODIS data. *Int. J. Remote Sens.* **2007**, *28*, 5079–5101. [CrossRef]
41. Hu, X.; Xu, H. A new remote sensing index for assessing the spatial heterogeneity in urban ecological quality: A case from Fuzhou City, China. *Ecol. Indic.* **2018**, *89*, 11–21. [CrossRef]
42. Wang, L.; Jiao, L.; Lai, F.; Zhang, N. Evaluation of ecological changes based on a remote sensing ecological index in a Manas Lake wetland, Xinjiang. *Acta Ecol. Sin.* **2019**, *39*, 2963–2972.
43. Xu, C.; Li, B.; Kong, F.; He, T. Spatial-temporal variation, driving mechanism and management zoning of ecological resilience based on RSEI in a coastal metropolitan area. *Ecol. Indic.* **2024**, *158*, 111447. [CrossRef]
44. Yao, Y.; Liu, Y.; Wang, Y.; Fu, B. Greater increases in China's dryland ecosystem vulnerability in drier conditions than in wetter conditions. *J. Environ. Manag.* **2021**, *291*, 112689. [CrossRef]
45. Peng, S.; Ding, Y.; Wen, Z.; Chen, Y.; Cao, Y.; Ren, J. Spatiotemporal change and trend analysis of potential evapotranspiration over the Loess Plateau of China during 2011–2100. *Agric. For. Meteorol.* **2017**, *233*, 183–194. [CrossRef]
46. Li, B.; Gui, D.; Xue, D.; Liu, Y.; Ahmed, Z.; Lei, J. Analysis of the Expansion Characteristics and Carrying Capacity of Oasis Farmland in Northwestern China in Recent 40 Years. *Agronomy* **2022**, *12*, 2448. [CrossRef]
47. Wang, J.; Zhang, F.; Jim, C.-Y.; Chan, N.W.; Johnson, V.C.; Liu, C.; Duan, P.; Bahtebay, J. Spatio-temporal variations and drivers of ecological carrying capacity in a typical mountain-oasis-desert area, Xinjiang, China. *Ecol. Eng.* **2022**, *180*, 106672. [CrossRef]
48. Zhang, H.; Wang, W.; Wang, J.; Zhao, X.; Hou, Y.; Bo, Y. Analysis on Evolution of Ecological Vulnerability of Shanxi Province based on the Remote Sensing and GIS Technique. *Remote Sens. Technol. Appl.* **2024**, *39*, 478–491. [CrossRef]
49. Xu, M.; Luo, J.; Cui, C. Oasis agriculture sustainable development in Xinjiang. *J. Arid Land. Res. Environ.* **2011**, *25*, 20–23.
50. Zhang, J.; Ji, X.; Chen, X.; Xu, S.; Jiao, D. Regional supply-demand balance and carrying capacity of water resources for Linze Oasis in the middle of Hexi Corridor. *Arid Land Geogr.* **2018**, *41*, 38–47. [CrossRef]
51. Xiong, H.; Fu, J.; Wang, K. Evaluation of water resource carrying capacity of Qitai Oasis in Xinjiang by entropy method. *Chin. J. Eco-Agric.* **2012**, *20*, 1382–1387. [CrossRef]

52. Xu, D.; Wang, Y.; Wang, J. A review of social-ecological system vulnerability in desertified regions: Assessment, simulation, and sustainable management. *Sci. Total Environ.* **2024**, *931*, 172604. [CrossRef] [PubMed]
53. Yang, Q.; Chen, Y.; Li, X.; Yang, J.; Gao, Y. Livelihood Vulnerability and Adaptation for Households Engaged in Forestry in Ecological Restoration Areas of the Chinese Loess Plateau. *Chin. Geogr. Sci.* **2024**, *34*, 849–868. [CrossRef]
54. Yao, J.; Li, M.; Dilinuer, T.; Chen, J.; Mao, W. The assessment on "warming-wetting" trend in Xinjiang at multi-scale during 1961–2019. *Arid Zone Res.* **2022**, *39*, 333–346.
55. Fan, L.; Wu, Y.; Chi, H.; Zheng, S.; Yan, J.; Ren, Y.; Sun, Z. Detecting Spatiotemporal Changes of Freshwater in Northwest China under a Warm-Wetting Climate using Remote Sensing. *J. Geo-Inf. Sci.* **2023**, *25*, 1842–1854.
56. Yao, J.; Mao, W.; Chen, J.; Dilinuer, T. Signal and impact of wet-to-dry shift over Xinjiang, China. *Acta Geogr. Sin.* **2021**, *76*, 57–72.
57. Ding, Y.; Liu, Y.; Xu, Y.; Wu, P.; Xue, T.; Wang, J.; Shi, Y.; Zhang, Y.; Song, Y.; Wang, P. Regional Responses to Global Climate Change: Progress and Prospects for Trend, Causes, and Projection of Climatic Warming-Wetting in Northwest China. *Adv. Earth Sci.* **2023**, *38*, 551–562.
58. Ouyang, Z.; Zhao, T.; Wang, X.; Miao, H. Ecosystem services analyses and valuation of China terrestrial surface water system. *Acta Ecol. Sin.* **2004**, *24*, 2091–2099.
59. Han, B.P. Reservoir ecology and limnology in China: A retrospective comment. *Sci. Limnol. Sin.* **2010**, *22*, 151–160.
60. Li, J.; Chen, G.; Huang, L.; Kong, L.; Suo, Q.; Wang, X.; Zhu, Y.; Zhang, T.; Wang, L. Environmental changes and cladoceran community responses during the past 200 years in an alpine lake of Wodi Co, Northwest Yunnan. *J. Lake Sci.* **2023**, *35*, 2170–2184.
61. Zhang, Y.; Li, H.; Wu, L. Change Features and Influencing Factors of Trophic States of the Caotang River in Three Gorges Reservoir. *Ecol. Environ. Sci.* **2020**, *29*, 2060–2069.